Analysis of Virtual Inertia Control Implementation Based on Redox Flow Batteries for Frequency Stability in Low Inertia Power Systems

Herlambang Setiadi [1], Ismayahya Ridhan Mutiarso [2], Feby Ananta Sari [3]

[1,2,3] Faculty of Advanced Technology and Multidiscipline, Universitas Airlangga, Indonesia

h.setiadi@ftmm.unair.ac.id

Abstract. Integration of renewable energy sources into power systems often poses challenges in system stability, particularly frequency stability. Excessive frequency fluctuations can lead to disruptions in the electrical grid, causing equipment damage and system failures. Therefore, precise control mechanisms are essential to maintain frequency stability. In this research, redox flow batteries (RFB) are utilized as frequency regulation systems in a two-area power system with low inertia. The research analyzes the impact of photovoltaic solar integration on a two-area power system and evaluates the use of virtual inertia control based on redox flow batteries for frequency stability enhancement using Matlab Simulink. This study analyzes the effect of solar power integration on a two-area power system and the use of virtual inertia control (VIC) based on redox flow batteries (RFB) on system frequency stability. Three case studies were conducted in this research. The first case is a two-area power system with a 0.3 p.u. load change in area 1. Case 2 is the system in case 1 with the addition of PV in area 1, and case 3 is the system in case 1 with the addition of virtual inertia control based on redox flow batteries. In the analysis result, the integration of PV in the system causes a significant frequency spike, with the nadir frequency in area 1 reaching 61.57 Hz. While the addition of RFB-based VIC can reduce the impact of PV integration and maintain frequency stability with the nadir frequency in area 1 at 60.21 Hz.

Keywords: Frequency Stability, Redox Flow Batteries, Photovoltaic Solar Integration, Virtual Inertia Control, MATLAB Simulink.

1 Introduction

Fossil fuels such as petroleum, natural gas, and coal currently dominate as primary energy sources. However, their utilization has resulted in significant environmental repercussions, including air pollution, greenhouse gas emissions, and global climate change [1][2]. Consequently, the development of environmentally friendly alternative energy sources is imperative. Renewable energy, derived from natural resources such as solar, wind, hydro, and geothermal, has gained increasing prominence. This is evidenced by the widespread adoption of technologies like electric vehicles, LED lighting, and various energy efficient devices. Nevertheless, renewable energy sources, particularly solar photovoltaic (PV) and wind turbines, encounter challenges

© The Author(s) 2024
T. Amrillah et al. (eds.), *Proceedings of the International Conference on Advanced Technology and Multidiscipline (ICATAM 2024)*, Advances in Engineering Research 245,
https://doi.org/10.2991/978-94-6463-566-9_2

concerning system stability. Solar PV plants, unlike conventional power plants, lack rotating machinery. Instead, they employ inverters to convert direct current (DC) to alternating current (AC), substituting the synchronous machines typically used in conventional power generation [3][4]. This substitution introduces challenges, as it can lead to instability and disruptions within the power system [4]. System instability arises due to the variable power output from PV sources, influenced by the intermittent nature of solar energy. Moreover, the replacement of synchronous machines with inverters results in reduced system inertia [5]. Previous studies have demonstrated that low inertia exacerbates frequency fluctuations and power imbalances, leading to system instability and potential frequency oscillations [6].

To mitigate these issues, supplementary systems are essential for maintaining system stability. Energy storage systems can be deployed to stabilize low inertia systems by providing a power smoothing effect, particularly in solar and wind energy generation [7]. One viable approach involves the utilization of redox flow batteries (RFB) for energy storage. RFBs consist of electrolyte solutions stored in two tanks and a cell stack that allows for the separation of energy and power [8]. Research has highlighted the advantages of RFBs, including safe operation, long cycle life, and flexible power capacity [9].

Therefore, incorporating additional controllers in energy storage systems is necessary to address the challenges of low inertia systems. Virtual inertia control presents a solution to enhance frequency stability in low inertia systems by simulating the effect of synchronous inertia without the need for actual synchronous machines [10]. This study proposes the design of a virtual rotor based on RFBs for frequency regulation in low inertia power systems. The objective is to mitigate the impact of low inertia on system stability. The research includes an analysis and comparison of the effects of implementing RFB based virtual inertia control versus systems without such control.

2 Literature Review

2.1 Virtual Inertia Control

Virtual Inertia Control (VIC) operates by mimicking the inertia characteristics produced by traditional synchronous machines through the application of vibration equations that represent the characteristics of synchronous machines without rotating mass. VIC serves as an additional inertia power controller needed by the system [11]. In renewable energy systems, such as photovoltaic (PV) power plants, the absence of synchronous machines results in low inertia production. This condition impacts frequency stability, causes issues with power quality, and reduces system flexibility [12]. To address these issues, VIC is implemented to enhance and maintain system stability and reliability through frequency regulation. One method used in the implementation of virtual inertia is differentiation, which is employed to calculate frequency changes and add inertia to the system to stabilize the frequency [13]. Generally, the inertia output can be expressed as

$$\Delta P_{VI} = \left(\frac{J_{VI}\left(\frac{d\Delta f}{dt}\right) + D_{VI}(\Delta f)}{R_{VI}} \right) \quad (1)$$

This equation reflects how VIC uses virtual inertia and damping to generate power that stabilizes the system frequency. The equation (1) explains that ΔPvi is an inherited force of virtual inercia control. (VIC). *Jvi* is the constant of inertia that reflects the system's response to frequency change *(*Δf*)*. *(*$\Delta f/dt$*)* indicates the rate of frequencies change, whereas D*vi* measures the reduction of the system. R*v*i is a constant that connects the change in frequences to an artificial inertial force, affecting its impact on the systems. $\Delta Pstorage$ is the power contribution of the energy storage system toining frequency stability.

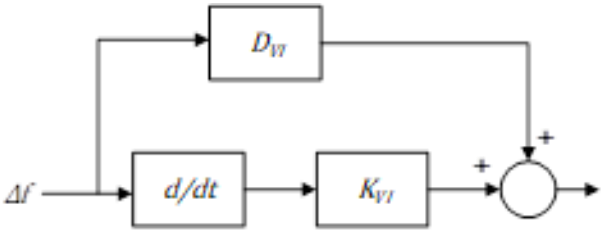

Fig. 1 Block Diagram of Virtual Inertia Control

Figure 1 illustrates the dynamic modeling to analyze the transient frequency response. VIC is used to reduce frequency overshoot, whereas virtual damping is applied to quickly restore frequency stability after the integration of renewable energy sources [14]. Virtual damping emulates the effect of damper windings in synchronous generators, helping to dampen frequency oscillations following disturbances.

2.2 **Redox Flow Batteries**

A Redox Flow Battery (RFB) consists of an electrolyte liquid stored in two separate tanks, each containing an electrolyte solution and a cell stack that allows for the separation of energy and power. The two tanks serve as the anode and cathode, respectively, with a membrane separating the anode and cathode tanks. The electrolyte is pumped from the tanks to the cell stack through pipes equipped with two pumps. Within the cell stack, a chemical reaction occurs that converts electrical energy into chemical energy and vice versa [15]. The RFB responds more quickly to disturbances than a governor because it undergoes frequent charging and discharging, which helps to mitigate peak frequency deviations when the load changes suddenly [16]. Because of its faster response compared to a governor input, the RFB is considered an active power source with a time constant T_{rfb}. The block diagram of the RFB is shown in figure 2, and the operation of the RFB unit within the system is illustrated by equation (2).

$$\left\{\left(ACE \times K_{rfb}\right) - \left(\frac{K_{ri}}{1+sT_{ri}}\right)\right\}\left(\frac{K_{ri}}{1+sT_{ri}}\right) - (setvalue) = \Delta P_{rfb} \quad (2)$$

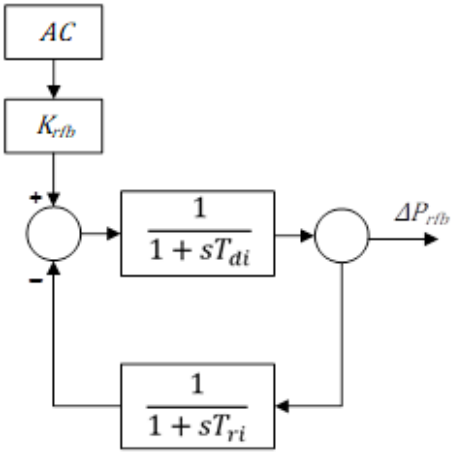

Fig. 2 Block Diagram of Virtual Inertia Control

2.3 Frequency Standard

The frequency standards referenced are based on IEEE, the Institute of Electrical and Electronics Engineers, C37.102-2006, which is a revision of ANSI/IEEE C37.106-2003 [17]. This standard applies to systems with a base frequency of 60 Hz and defines frequency limits across three categories. The first category, Prohibited Operation, includes frequencies outside the normal range that are forbidden for operation due to potential damage to equipment or systems, such as frequencies above 61.5 Hz or within the range of 57.67 Hz to 58.17 Hz. The second category, Continuous, allows frequencies within the range of 59.58 Hz to 60.42 Hz for continuous operation without time constraints. This range is considered optimal for stable and reliable performance without disrupting other equipment. The third category, Restrictive Operation, includes frequencies that are permitted with specific time limitations, such as frequencies between 58.17 Hz to 59.58 Hz and 60.42 Hz to 61.50 Hz. These frequencies are allowed only for certain durations to maintain system performance, safety, and stability. Each category provides essential guidelines to ensure effective and safe system operation.

3 Method

The method used in the study is dynamic modeling for a two-area connected system. This method involves the use of Matlab Simulink software designed to dynamically model the electrical system. A two-area power system is a system consisting of two control areas connected by a tie line reactance (Xtie).

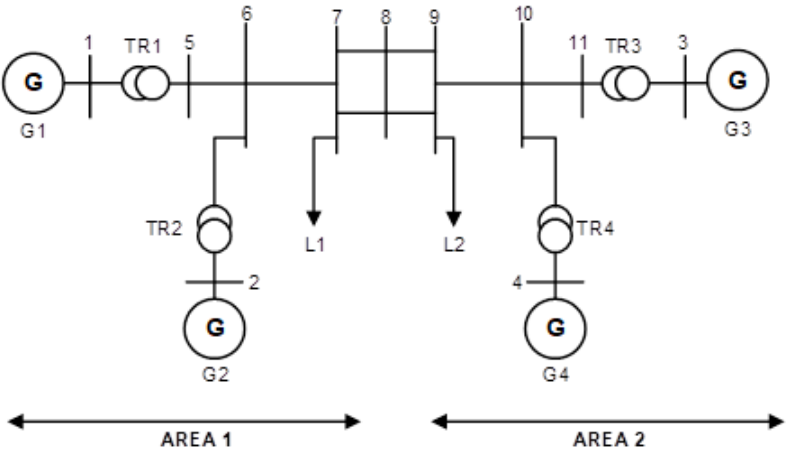

Fig. 3 Dynamic Modeling of a Two-Area Interconnected System

Table 1 Parameters of the Two-Area Interconnected System**.**

Parameters	Area 1	Area 2
Ki(s)	0,3	0,3
R (Hz/p.u.MW)	0.05	0.0625
β (p.u.MW/Hz)	20,6	16,9
D (s)	0,6	0,9
H (s)	5	4
Tg (s)	0.2	0.3
Tt (s)	0.5	0.6
PL (p.u.MW/Hz)	2	2

In this study, the modeling of the interconnected two-area power system was carried out using the parameter data in table 1. In the first case, the modeling of the two-area system was simulated by providing a disturbance in the form of load shedding in area 1 and then analyzing the frequency output. This case is a basic case without any additions, either solar power plant, energy storage, or virtual inertia control. This case was carried out to determine the frequency output produced before the solar power plant integration was carried out and to compare and analyze the results with the system with solar power plant integration. The system modeling is shown in figure 4.

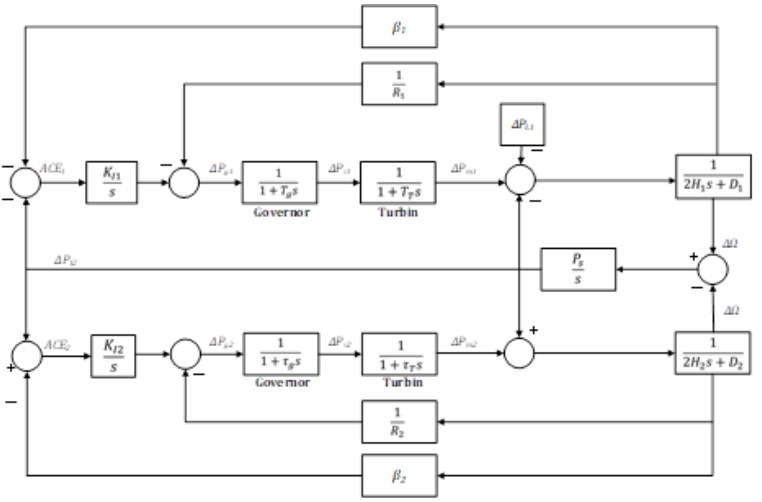

Fig. 4 Block Diagram of a Two-Area Interconnected System

In the second case, testing was carried out using a block diagram as in figure 5, where the solar power plant was integrated into area 1 of the previously modeled two-area interconnected power system. This case was carried out to determine the frequency output produced after the solar power plant integration was carried out and to compare and analyze the results with the system without solar power plant integration. The magnitude of the frequency drop and overshoot was then analyzed and compared with case 1 to determine and understand the impact of the solar power plant integration on the system.

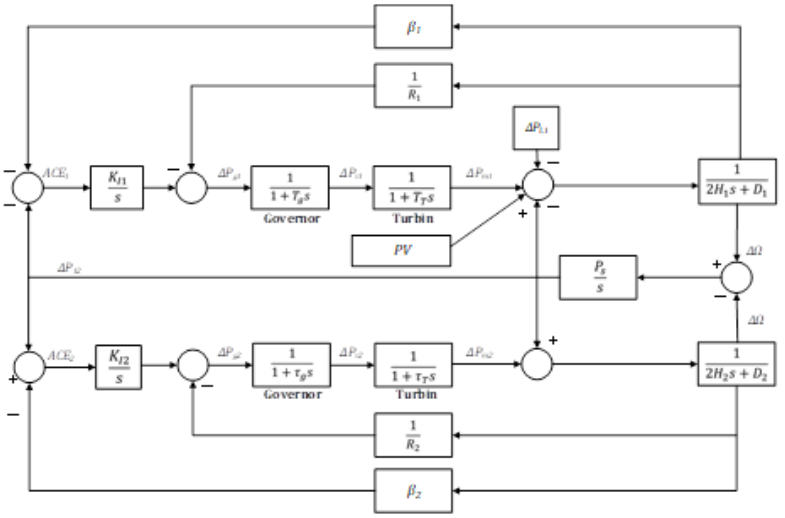

Fig. 5 Block Diagram of a Two-Area System with Integrated PV Power Plant

Then in the third case, testing was carried out by installing virtual inertia control based on redox flow batteries (RFB) on the system to reduce the impact of inertia reduction due to solar power plant integration. Integrating a PV system into the system in area 1 will result in a decrease in system inertia, which can disrupt frequency stability. The installation of energy storage in the form of redox flow batteries is expected to help reduce the frequency drop in the system. This is because the energy storage will supply active power to the system, aiding in the stabilization of system frequency. Redox flow batteries are expected to help stabilize the frequency by supplying active power to help stabilize the system frequency. The parameters for redox flow batteries are listed in table 2.

Table 2. Virtual Inertia Control Parameters Based on Redox Flow Batteries

Parameters	Area 1
D_{VI}	45
K_{VI}	10
K_{RFB}	1,8
T_{di}	0,01
T_{ri}	0,01

Virtual inertia control modeling based on redox flow batteries is modeled as shown in figure 6. The block diagram with solar power plant integration and additional virtual inertia control based on redox flow batteries is shown in figure 7. The analysis was carried out on the system frequency response in all three cases to assess the system's ability to maintain and improve frequency stability.

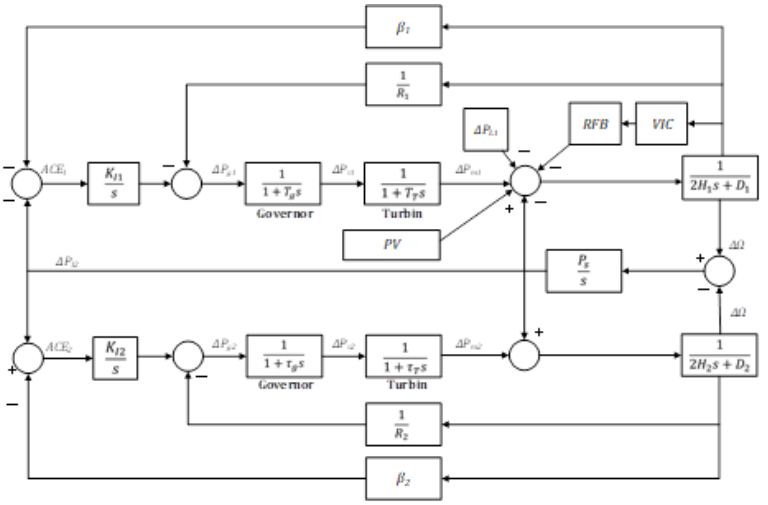

Fig. 6 Block Diagram of a Two-Area Low-Inertia System with VIC Based on RFB

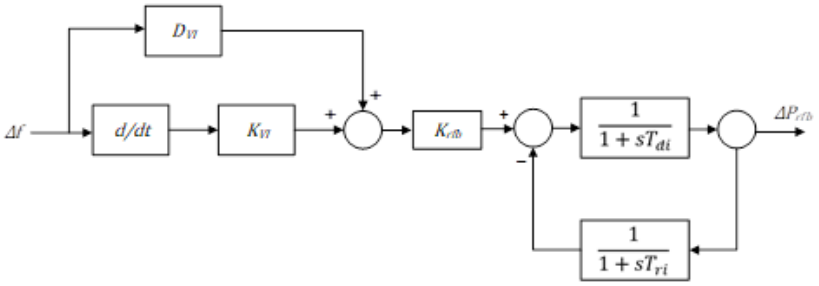

Fig. 7 Block Diagram of VIC Based on RFB

4 Result

4.1 Frequency Response Test Results

The first case study involved testing a two-area interconnected power system with a disturbance in the form of a 0.3 p.u. load shedding in area 1. The research results in figure 8(a) show that the system frequency increased to 61.23 Hz after the disturbance, which falls into the overfrequency condition and is categorized as restricted operation according to IEEE Std. The frequency returned to its original point after approximately 19.4 seconds. In area 2, the frequency fluctuated with an overshoot up to 60.29 Hz, but this increase was not as pronounced as in area 1, due to the load shedding occurring only in area 1. Nevertheless, the disturbance in area 1 also affected area 2, though less significantly. This conventional system, with its high inertia, helps to mitigate frequency fluctuations and is supported by two control systems: a primary control operating within 20-40 seconds and a secondary control functioning for up to 30 minutes, to maintain frequency stability. However, the results indicate that the system could not fully address the load shedding disturbance promptly.

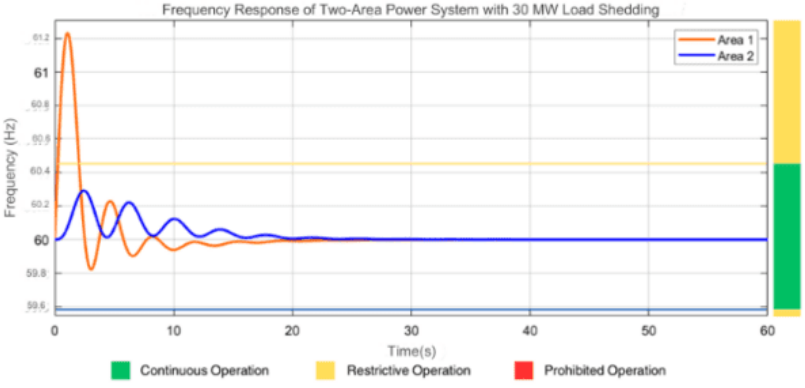

(a)

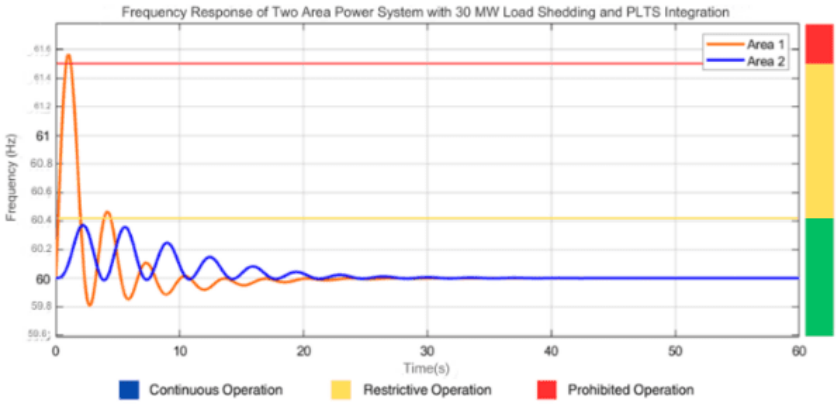

(b)

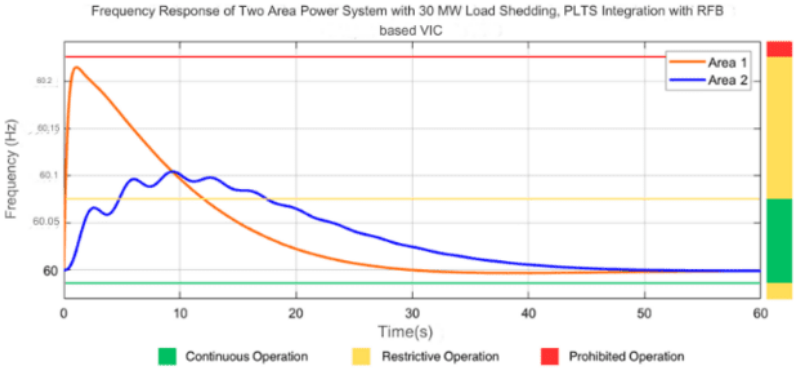

(c)

Figure. 8 Frequency Response: (a) case 1 (b) case 2 (c) case 3

In the second case study, an interconnected two-area power system was tested with a disturbance in the form of a 0.3 p.u. load shedding in area 1, similar to the first case study. However, this time, the system was also integrated with a solar power plant, which was considered as a step input into the system. This integration caused the system to have low inertia, leading to frequency fluctuations. The research results in figure 8(b) show that integrating the SPP at 0.2 p.u. into the conventional power system caused the highest frequency spike to reach 61.56 Hz in area 1 within 0.98 seconds, and 60.37 Hz in area 2 within 2.13 seconds. According to IEEE Std, the frequency spike in area 1 was classified as overfrequency and falls under the prohibited operation category, meaning frequencies above 61.5 Hz are prohibited even for a few seconds. The frequency fluctuations began to normalize after 22.7 seconds. In area 2, the frequency spike was at 60.37 Hz, which is still within the continuous operation range and considered safe. Although area 2 did not experience load shedding or solar power plant integration, fluctuations in area 1 affected area 2 due to the interconnected system. This

test demonstrates that integrating a solar power plant into an interconnected two-area power system can adversely affect frequency stability, caused by load and generation imbalances and the weakening of system inertia.

In case 3, the power system was tested with the addition of redox flow batteries (RFB) and virtual inertia control (VIC) to address the significant frequency fluctuations from the previous case. The addition of RFB and VIC effectively reduced frequency spikes, with the nadir frequency in Area 1 at 60.21 Hz and the highest spike in area 2 at 60.10 Hz. As shown in figure 8(c), the results placed the frequency in the continuous operation category, indicating stable system performance and normal operation without time constraints.

Table 3. Frequency response results for case 1, case 2, and case 3

Case	Condition	Nadir Frequency (Hz)	
		Area 1	Area 2
Case 1	30 MW load shedding	61,23	60,29
Case 2	30 MW load shedding Solar power plant integration 0.2 p.u.	61,57	60,37
Case 3	30 MW load shedding Solar power plant integration 0.2 p.u. Addition pf VIC based RFB	60,21	60,10

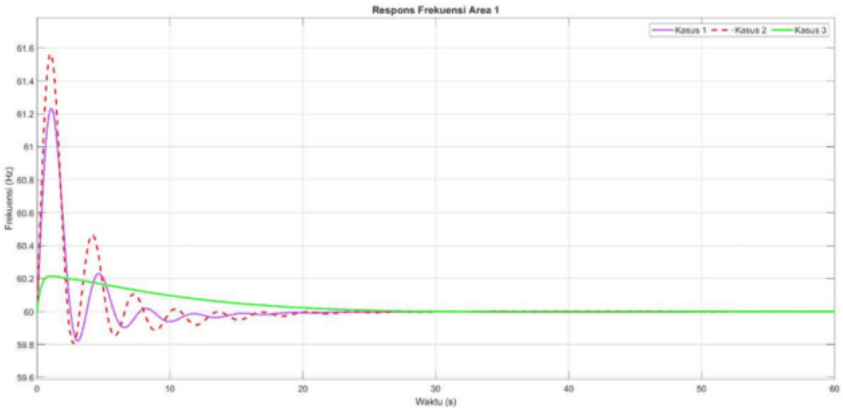

(a)

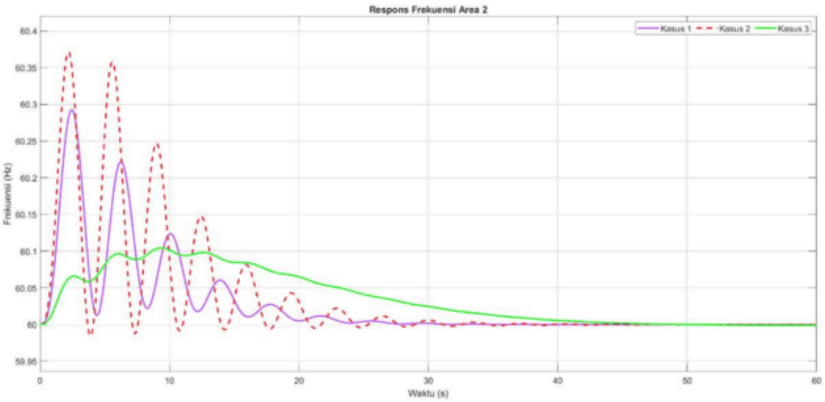

(b)

Fig. 9 Frequency Response: (a) area 1 (b) area 2

From the three cases conducted, case 1 showed a frequency spike due to load shedding in Area 1. In case 2, PV integration caused a higher frequency spike due to generation imbalance. To address this, redox flow batteries with virtual inertia control were used. As shown in figure 9(a), VIC based on RFB improved frequency stability by reducing spikes caused by disturbances. In area 2, figure 9(b) shows that case 1 had a frequency rise to 61.23 Hz, within the continuous operation range. Case 2 showed a spike up to 60.37 Hz with oscillations. Case 3, using VIC based on RFB, reduced spikes and oscillations, with a frequency rise to 60.10 Hz. The results indicate that VIC based on RFB is effective in minimizing frequency spikes and maintaining stability.

4.2 Mechanical power response of the system

Frequency stability can impact mechanical power in the system. Figure 10 illustrates mechanical power in each area across different cases. In case 1, there is a reduction in system mechanical power due to a disturbance from a 0.3 p.u. load shedding. In Area 1, the mechanical power drops to 56 MW, then oscillates before stabilizing at 70 MW. In Area 2, the power decreases to 93 MW, followed by oscillation, and finally stabilizes at 100 MW after 32.15 seconds. This decrease is due to a frequency spike affecting the mechanical power needed to maintain frequency stability following the load shedding. In Case 2, the integration of PV systems causes an imbalance between generation and load, leading to a drop in mechanical power required in Area 1 to 47.2 MW, which then oscillates and stabilizes at 60 MW. In Area 2, the drop in mechanical power is more significant than in Case 1, reaching 91.5 MW, oscillating, and stabilizing at 100 MW after 29.42 seconds.

In Case 3, the mechanical power reduction in Area 1 occurs gradually until it stabilizes at 60 MW. In Area 2, the reduction is gradual until 97.2 MW with minor oscillations before stabilizing at 100 MW after 47.24 seconds. The use of VIC based on RFB demonstrates the ability to maintain system frequency and improve stability, as indicated by a gradual decrease in mechanical power without excessive drops and oscillations.

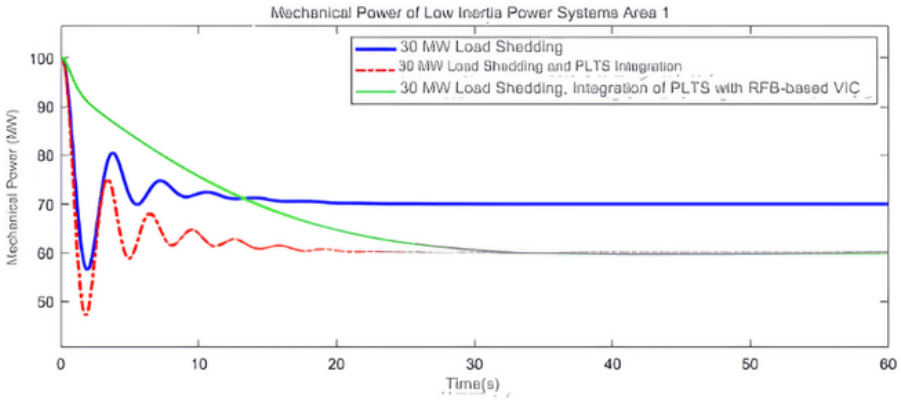

(a)

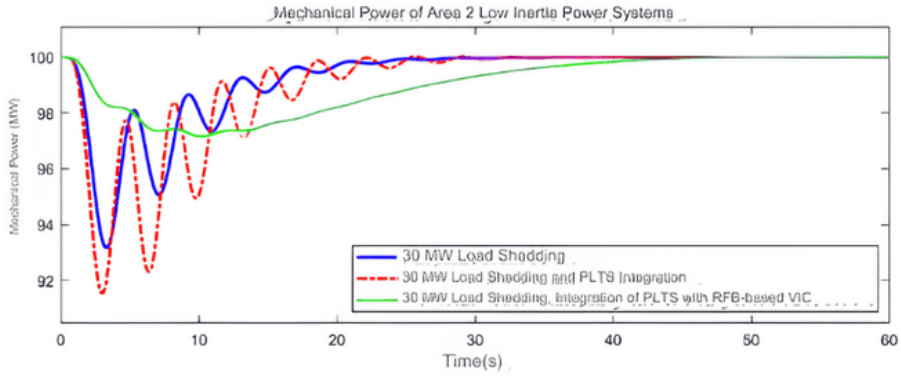

(b)

Fig. 10 Mechanical Power Response: (a) area 1 (b) area 2

5 Conclusion

The integration of solar power plants into the interconnected two-area power system can have a significant impact on the system frequency response. The addition of solar power plants can cause frequency fluctuations reaching 61.57 Hz in area 1 and 60.37 Hz in area 2. This occurs because the characteristics of solar power plant are not constant and do not have inertia control like conventional power plants so they cannot adjust power when there is a disturbance in the system. Comparison of the system frequency response results before and after the use of Virtual Inertia Control (VIC) based on Redox Flow Battery (RFB) shows a significant difference. In case 1, the system frequency experienced a spike reaching 61.23 Hz, which is categorized as restrictive operation. Case 2 showed a higher frequency spike, reaching 61.57 Hz, and fell into the prohibited operation category. In contrast, case 3 experienced a relatively small frequency spike, namely 60.21 Hz, which is still categorized as continuous operation. Thus, it can be concluded that the addition of RFB-based VIC plays an

important role in maintaining frequency stability in the interconnected two-area power system, especially in dealing with conditions with low inertia.

Acknowledgments. The authors would like to thank Airlangga University for their support and assistance in publishing this journal. We also greatly appreciate the contributions and assistance from all parties involved in this research**.**

References

1. A. T. Mulyono, "The Sustainability of Fossil Energy Development in Indonesia: Heading to Awry and Backfires Policy?" in Proc. 3rd Int. Conf. Law Governance (ICLAVE 2019), Atlantis Press, 2020, pp. 138-144.
2. A. R. Ridzuan, A. Albani, A. R. A. Latiff, M. I. M. Razak, and M. H. Murshidi, "The impact of energy consumption based on fossil fuel and hydroelectricity generation towards pollution in Malaysia, Indonesia and Thailand," Int. J. Energy Econ. Policy, vol. 10, no. 1, pp. 215-227, 2020.
3. P. Tielens and D. Van Hertem, "The relevance of inertia in power systems," Renew. Sustain. Energy Rev., vol. 55, pp. 999-1009, 2016.
4. T. Kerdphol, F. S. Rahman, M. Watanabe, and Y. Mitani, "Robust Virtual Inertia Control of a Low Inertia Microgrid Considering Frequency Measurement Effects," IEEE Access, vol. 7, pp. 57550-57560, 2019, doi: 10.1109/ACCESS.2019.2913042.
5. A. S. Surya, M. P. Marbun, M. Marwah, K. G. H. Mangunkusumo, B. B. S. Harsono, and H. B. Tambunan, "Study of Synchronous Condenser Impact in Jawa-Madura-Bali System to Provide Ancillary Services," in 2020 12th Int. Conf. Inf. Technol. Elect. Eng. (ICITEE), IEEE, 2020, pp. 234-238.
6. K. S. Ratnam, K. Palanisamy, and G. Yang, "Future low-inertia power systems: Requirements, issues, and solutions - A review," Renew. Sustain. Energy Rev., vol. 124, 2020, doi: 10.1016/j.rser.2020.109773.
7. D. Lamsal, V. Sreeram, Y. Mishra, and D. Kumar, "Output power smoothing control approaches for wind and photovoltaic generation systems: A review," Renew. Sustain. Energy Rev., vol. 113, 2019, doi: 10.1016/j.rser.2019.109245.
8. L. Wang, H. Y. Gao, C. W. Tseng, Z. H. Huang, M. F. Lee, Y. S. Lin, H. S. Huang, C. C. Tseng, A. V. Prokhorov, H. Bin Mokhlis, K. H. Chua, and M. Tripathy, "Small-Signal Stability Analysis of a Vanadium Redox Flow Battery-based Energy-Storage System," in 2021 IEEE Int. Future Energy Electron. Conf., IFEEC 2021, 2021, pp. 1-6, doi: 10.1109/IFEEC53238.2021.9661934.
9. M. M. Hiksas and M. L. Aninditio, "Redox Flow Batteries for small scale energy storage," in 2016 IEEE Conf. Technol. Sustain., SusTech 2016, 2017, pp. 134-139, doi: 10.1109/SusTech.2016.7897155.
10. H. Setiadi, R. Shah, M. R. Islam, D. A. Asfani, T. H. Nasution, M. Abdillah, P. Megantoro, and A. U. Krismanto, "An Extreme Learning Machine Based Adaptive VISMA for Stability Enhancement of Renewable Rich Power Systems," Electronics (Switzerland), vol. 11, no. 2, 2022, doi: 10.3390/electronics11020247.
11. B. N. Syifa, D. A. Asfani, A. Priyadi, and H. Setiadi, "Frequency Stability Analysis on Optimization of Virtual Inertia Controller Settings Based on Retired Electric Vehicles Battery Using Firefly Algorithm," in Proc. Int. Conf. Computer Eng., Network and Intelligent Multimedia (CENIM 2022), Vic, 2022, pp. 365–370. [Online]. Available: https://doi.org/10.1109/CENIM56801.2022.10037414

12. J. Fang, H. Li, Y. Tang, and F. Blaabjerg, “On the Inertia of Future More-Electronics Power Systems,” IEEE J. Emerg. Sel. Topics Power Electron., vol. 7, no. 4, pp. 2130–2146, 2019. [Online]. Available: https://doi.org/10.1109/JESTPE.2018.2877766
13. A. N. A. Maulidhia, D. A. Asfani, A. Priyadi, and H. Setiadi, “Frequency Stability Analysis on Optimization of Virtual Inertia Control (VIC) Capacitor Energy Storage (CES) Controller Settings Using Particle Swarm Optimization,” in Proc. Int. Conf. Computer Eng., Network and Intelligent Multimedia (CENIM 2022), 2022, pp. 359–364. [Online]. Available: https://doi.org/10.1109/CENIM56801.2022.10037313
14. T. Kerdphol, F. S. Rahman, M. Watanabe, and Y. Mitani, “Virtual Inertia Synthesis and Control,” in Power Systems. [Online]. Available: https://link.springer.com/book/10.1007/978-3-030-57961-6
15. R. D’Agostino, L. Baumann, A. Damiano, and E. Boggasch, “A Vanadium-Redox-Flow-Battery Model for Evaluation of Distributed Storage Implementation in Residential Energy Systems,” IEEE Trans. Energy Convers., vol. 30, no. 2, pp. 421–430, 2015. [Online]. Available: https://doi.org/10.1109/TEC.2014.2369437
16. H. Setiadi, N. Mithulananthan, and M. J. Hossain, “Impact of Battery Energy Storage Systems on Electromechanical Oscillations in Power Systems,” 2017.
R. Shankar, K. Chatterjee, and R. Bhushan, “Impact of Energy Storage System on Load Frequency Control for Diverse Sources of Interconnected Power System in Deregulated Power Environment,” Int. J. Electr. Power Energy Syst., vol. 79, pp. 11–26, 2016. [Online]. Available: https://doi.org/10.1016/j.ijepes.2015.12.029

Open Access This chapter is licensed under the terms of the Creative Commons Attribution-NonCommercial 4.0 International License (http://creativecommons.org/licenses/by-nc/4.0/), which permits any noncommercial use, sharing, adaptation, distribution and reproduction in any medium or format, as long as you give appropriate credit to the original author(s) and the source, provide a link to the Creative Commons license and indicate if changes were made.

The images or other third party material in this chapter are included in the chapter's Creative Commons license, unless indicated otherwise in a credit line to the material. If material is not included in the chapter's Creative Commons license and your intended use is not permitted by statutory regulation or exceeds the permitted use, you will need to obtain permission directly from the copyright holder.